

NMR RELAXIVITY GROUPING OR NMR FACIES IDENTIFICATION IS KEY TO EFFECTIVE INTEGRATION OF CORE NUCLEAR MAGNETIC RESONANCE DATA WITH WIRELINE LOG

Henry A. Ohen, Paulinus M. Enwere, and Jerry Kier, Core Laboratories

ABSTRACT

Interpretation of nuclear magnetic resonance (NMR) logs is challenged by the following three factors: (1) incorrect critical transverse relaxation time (T_2) cutoff for free fluid index (2) incorrect permeability model and (3) effect of unusual relaxation properties of the rock. Some of these challenges can be addressed through the use of NMR core spectrometry data for log calibration. However, further difficulty lies in the application of the NMR core data to correctly calibrate wireline NMR logs.

In this work, we demonstrate that identification and delineation of NMR “relaxivity groups” or “NMR facies” are critical in the application of laboratory NMR calibration data to log analysis. We define NMR facies or relaxivity groups as units in the reservoir that have similar NMR relaxation characteristics. Hence, NMR relaxation characteristics such as T_2 cutoff and relaxivity constant can be averaged within each relaxivity group. The method presented also allows direct application of laboratory based models for log interpretation irrespective of tool dependent factors like logging speed, borehole conditions, fluid types and saturation.

Relaxivity group concept encompasses the following: (1) the fundamental physics of the behavior of the magnetic dipole of hydrogen nuclei in the presence of an applied (external) magnetic field, (2) the mathematical relationship between the relaxation rates of magnetization, the pore size that contain the liquid and other surface properties of the porous media, and (3) the mineralogical attributes of the rock formation. Therefore, combined influence of mineralogical and textural attributes on relaxation rate is captured.

Delineation of this group is based on NMR porosity and normalized median value of the relaxation time. These data can be obtained directly from wireline NMR log measurements.

The validity and applicability of the methodology is demonstrated by a regional study involving measurement of NMR transverse relaxation time constant (T_2) on about 400 plugs, and mineralogical, textural and pore size attributes on selected samples.

This work provides a sound basis for tool calibration and enhanced interpretation of NMR wireline log output and also an effective algorithm for permeability determination.

INTRODUCTION

Nuclear magnetic resonance logging has improved over the last few years due to improved tool design and the use of CPMG spin-echo method to measure true spin-spin relaxation (T_2) of formation fluids. This superior tool design has helped to overcome the initial challenges of doping the drilling mud. We are however faced with new challenges related to the proper interpretation of echoes and T_2 distribution to obtain the objective of the logs, which is the determination of petrophysical properties of the formation rock. These challenges may arise from incorrect critical T_2 cutoff for free fluid index determination, incorrect permeability model and/or effect of unusual relaxivity properties of the rock. These challenges can be addressed through correct use and application of NMR core spectrometry data for log calibration.

It is a common practice among log analysts to use a fixed T_2 cutoff (T_{2c}) to determine BVI from NMR logs. Usually a T_{2c} near 33 ms is used for sandstones and about 100 ms for carbonate system. This approach can be inappropriate for certain formations. Formation permeability predicted by the NMR log results has been found to be too low or too high in some cases compared to permeability measured on cores taken from the zones of interest when a fixed T_{2c} was used to establish BVI for the NMR log. Surface relaxivity is influenced by surface composition (paramagnetic ions and absorbed hydrophobic/hydrophilic compounds

etc.). Hence, the reasons for unusual relaxation properties of some formation rocks containing fluid include the amount and location of paramagnetic and ferromagnetic material in the rock, wettability alteration due to emulsifiers present in some types of mud systems and effects of vugs in carbonate systems. Emulsifiers are typically used in invert emulsion mud system to help make the drilled solids in the mud oil-wet for ease of lifting to the surface but may also change the wettability of the reservoir rock. The result is a change in the NMR response because the relaxation rate of an oil-held proton in contact with rock is slower than that of water-wet proton in contact with the rock. The end result is an under-estimated BVI and over estimated Permeability¹.

In an ideal case where there is uniform relaxivity in the rock system and a constant T_2 cutoff, there would be a defined relationship between NMR porosity and mean or median T_2 . A deviation from this trend indicates changes in relaxation characteristics and hence different NMR facies. Therefore, based on extensive laboratory study and observations, we developed the concept of relaxivity grouping to facilitate the development of a consistent method of using the NMR data to predict deviation from relaxivity group or NMR facies. The recognition of these facies in a rock system provides the basis for the application of the appropriate interpretative tools and models for the analysis of the logs.

A relaxivity group consists of zones in the formation with similar NMR characteristics. The relaxivity group concept is very much analogous to the hydraulic units² and the Petrofacies³ concept, which groups zones of similar fluid flow characteristics.

Calibration of NMR logging tools with Laboratory NMR core data has been shown⁴ to enhance the quality of petrophysical data (porosity, permeability, free fluid index) derived from NMR logs. However, incorrect application of core data in log calibration would obviously lead to errors in determining these parameters. For example, the T_{2c} used to determine bound and free fluids may be incorrect either because it was arbitrarily chosen or established in the laboratory on the basis of non-representative desaturation pressure or it was applied to NMR log of formations, which it did not represent. These sources of error can be eliminated using NMR laboratory measurements as described in this paper.

RELAXIVITY GROUPING TECHNIQUE –THEORETICAL BASIS

The following expression relating relaxation time and porosity has been developed previously^{4,5}.

$$\log T_2 = \log f_z + \log \left(\frac{1}{r_2 S_{gv}} \right) \quad (1)$$

Where,

T_2 = NMR transverse relaxation time, sec

ϕ_z = porosity group, fraction

ρ_2 = rock surface relaxivity, $\mu\text{m}^2/\text{sec}$

S_{gv} = specific rock surface area, μm^2

ϕ = porosity, fraction

and

$$f_z = \frac{f}{1-f} \quad (2)$$

Equation (1) forms the basis for the relaxivity group concept, which analogous to the hydraulic units concept², classifies samples that exhibit similar NMR relaxation (rock-fluid interaction) characteristics into groups. Average parameters for the group serve as calibration points for interpreting NMR logs. The factor $(1/\rho_2 S_{gv})$, which is often referred to as relaxivity product, represents both the relaxation power and textural attributes of the formation. As implied from equation (1), the log-log plot of T_2 versus ϕ_z would result in a slope line, and $1/\rho_2 S_{gv}$ would be constant for all data points that lie on the slope line.

Formation rock samples or intervals with similar NMR relaxation characteristics lend themselves to the same group with their log T_2 versus log ϕ_z data clustering around the intercepting slope line. We refer to the samples or intervals from a given formation or reservoir with similar NMR characteristics as belonging

to the same Relaxivity Group. A relaxivity group is characterized by an average of discrete values of $1/\rho_2 S_{gv}$ within that unit. Cluster analysis techniques may be used to identify the correct number of relaxivity groups (correct number of straight lines with 45° angle through the data scatter). The main benefit of this approach (unlike most laboratory-based models) is that the data needed for the relaxivity grouping can be obtained directly from NMR logs. Once a laboratory model is developed, T_2 and ϕ_{NMR} from logs are used directly in equation (1) to distinguish the groups on the basis of the factor $1/\rho_2 S_{gv}$.

LABORATORY DATA TO DEFINE THE GROUPING

The key to successful application of this technique is an extensive core analysis data to cover most or all of the major relaxivity groups present in the formation of interest. The following analyses are recommended on representative core samples. Samples 1.5" or longer are preferred in order to obtain end trims for some of the analyses.

- (1) Conventional porosity and Klinkenberg permeability at net overburden pressure
- (2) Mineralogy focusing on amount and location of paramagnetic and ferromagnetic minerals (end trim)
- (3) Mercury injection capillary pressure (end trim)
- (4) Centrifuge capillary pressure
- (5) Magnetic susceptibility
- (6) NMR T_2 measurement at fully saturated and desaturated conditions

Centrifuge capillary pressure data is used to determine the desaturation pressure required to obtain irreducible conditions. The mercury injection data are used for calibration required to relate pore size from NMR data to pore throat size as shown in the next section. The flow diagram given in Figure 1 is recommended as a guide for correct application of the methodology presented in this paper.

RELATING PORE SIZE TO PORE THROAT SIZES DISTRIBUTIONS

Pore size distribution is typically obtained from NMR T_2 using the surface relaxivity, ρ_2 . Therefore, knowledge of relaxivity group helps to determine and assign, ρ_2 for accurate determination of pore size distribution from NMR data. Rock pore shape varies, but for simplicity in computing S_{gv} , it has been assumed that pore throat is spherical in shape, and hence mean hydraulic radius r_{mh} has been related to S_{gv} and porosity as follows^{4,5,6}:

$$r_{mh} = \frac{r_i}{2} \quad (3)$$

and

$$S_{gv} = \frac{f_z}{r_{mh}} \quad (4)$$

Where, r_i is the pore throat radius.

Amaefule et al. demonstrated (with limited data) that a plot of r_{mh}/Φ_z versus a factor called flow zone indicator² (FZI) yields a straight line with a constant slope equal to the Kozeny-Carman term $-t\sqrt{F_s}$, i.e.,

$$FZI = \frac{1}{t\sqrt{F_s}} \frac{r_{mh}}{f_z} \quad (5)$$

Where, t and F_s represent the pore throat tortuosity and shape factor, respectively.

This observation was also supported by data published recently⁴. Figure 2 shows data from a Gulf of Mexico field that also validates this supposition. The FZI was obtained^{2,4,5} from core analysis data of porosity and permeability as follows:

$$0.0314 \sqrt{\frac{K}{f}} = FZI f_z \quad (6)$$

To accurately determine pore throat size distribution from NMR data, it is important to realize the variability of the pore size to pore throat size ratios from one rock type to another. For a simple spherical pore shape:

$$F_{sv} = \frac{3}{r_p} \quad (7)$$

Where, F_{sv} is the surface area S_p to volume ratio V_p of the pore space

r_p is the pore radius;

NMR T_2 distribution can be converted to pore size distribution using the following equation⁴:

$$T_2 = \frac{r_p}{3r_2} \quad (8)$$

Defining pore size to pore throat size r_t ratio as $R_{pt} = r_p/r_t$, equation 8 can be written as

$$T_2 = \frac{R_{pt}}{3r_2} r_t \quad (9)$$

By taking the logarithm of both sides of Eq. 9, the resulting equation is:

$$\log(T_2) = \log \frac{R_{pt}}{3r_2} + \log r_t \quad (10)$$

Log-log plot of T_2 versus r_t would yield values for $R_{pt}/3r_2$. From Equations 1, 4, 5 and 10, average values for r_2 , R_{pt} and S_{gv} can be determined per relaxivity group from routine core analysis, NMR core analysis, and mercury injection data for use in log interpretation.

EXPERIMENTAL VALIDATION

Two example studies are presented as validation of the methodology for identifying and characterizing relaxivity groups within a formation or reservoir. The first example is from Africa and the second example is from North America. In both examples, each plug sample was fully saturated and NMR measurements were made. Then the plugs were desaturated to a non-movable fluid content in a centrifuge at air-brine capillary pressure dictated by the capillary pressure characteristics of the rock. NMR measurements were then similarly made on the partially brine-saturated rock samples to determine the T_2 distributions, T_{2c} and the corresponding non-movable fluid content.

RESULTS OF EXAMPLE 1

Figure 3 shows the relaxivity groups obtained in the study using nearly 400 sandstone samples. The cores used in the study were taken from various wells throughout the region, and ranged from lithified to unlithified with depositional facies that include lagoon, wave-dominated delta, fluvial-dominated delta, interdistributary bay, open marine shelf, slope/basin submarine fan/apron, and turbidites. Eight relaxivity groups were identified, with the reservoir NMR characteristic quality decreasing from Group 1 to Group 8. The descriptive statistics for $1/\rho_2 S_{gv}$ per relaxivity group presented in Table 1 shows that average values of $1/\rho_2 S_{gv}$ increase with increasing quality, ranging from 0.011 s for Group 8 to 1.163 s for Group 1.

Calculation and values of r_2 , S_{gv} and R_{pt}

The relaxivity constant ρ_2 was quantified using the following equation relating reservoir quality index (RQI) to the NMR relaxation time (Ohen et. al, 1996, 1995)^{3, 4}:

$$r_2 = \frac{RQI}{T_2} t \sqrt{F_s} \quad (11)$$

The Kozeny-Carman constant $t\sqrt{F_s}$ was determined from Equation (5) as described earlier. The mean hydraulic radius r_{mh} was obtained from mercury injection capillary pressure measurements on 27 plugs representing all environments of deposition (EOD), hydraulic units, and the relaxivity groups present in the database. The plot of r_{mh}/f_z versus FZI, shown in Figure 4, yielded $t\sqrt{F_s} = 3.55$. The specific surface area S_{gv} was then calculated from the relaxivity product ($1/\rho_2 S_{gv}$) after determining ρ_2 . The results are presented in Table 2. RQI was calculated from core analysis data with equation (6).

NMR provides pore size information while mercury porosimetry provides pore throat information. Combination of both data offers the opportunity to relate the pore radius r_p obtained from NMR T_2 measurement to pore throat radius r_t . Mercury injection pore throat data was used to obtain the pore to throat ratio R_{pt} . The unit slope (arrowheaded) line through the data points of the log-log plot of T_2 versus r_t (Figure 5) intercepts the secondary r_t -axis (where $T_2=1$ s) at 100, hence $3\rho_2/R_{pt}$ equals 100 in accordance with equation (10), from which R_{pt} was calculated as presented in Table 2.

Cutoff Relaxation Time and Non-movable Porosity

NMR cutoff transverse relaxation time (T_{2c}) is the value of T_2 below which the pore surface to fluid volume ratios in the porous media are too high for the fluid to be producible at the prevailing capillary pressure in the reservoir. The area under the T_2 distribution for all T_2 values less than T_{2c} defines the bulk volume irreducible (BVI). In this example (the Africa study) T_{2c} measurements were made on 136 samples that were representative of the eight relaxivity groups. The T_{2c} values were found to range from 3 ms to 70 ms. The T_{2c} data is presented in Table 2 from which it can be seen that average values of T_{2c} per relaxivity group increase with increasing relaxivity product, $1/\rho_2 S_{gv}$ (which is the NMR characteristic quality indicator).

For the purpose of assigning NMR T_2 cutoff calibration points (for log interpretation), all the samples used in this example were broadly classified into four environments of deposition; and the legends in Figure 6 are abbreviations as follows:

1. Channels – distributary (DC), tidal (TC), fan (FC), levee and distributary mouth bar (DMB).
2. Upper/middle shoreface (UMS) - upper, upper/middle, middle/upper and middle.
3. Lower/middle shoreface (LMS) - lower, lower/middle and middle/lower.
4. The rest (Other) - distal bar, prodelta, shelf, interdistributary bay, lagoon pond, slope/basin.

NMR T_{2c} values determined on representative channel sands range from 6 ms to 70 ms, averaging 23 ms; and from 3 ms to 60 ms, averaging 22 ms in the upper/middle shoreface. For the lower/middle shoreface, T_{2c} values range from 6 ms to 25 ms, averaging 13 ms; and for the rest, T_{2c} values range from 8 ms to 30 ms, averaging 16 ms.

Relationships to EOD, Mineralogical and Textural Attributes

Figure 6 shows the relationship between the depositional facies and the NMR facies. Relaxivity groups 1 through 5, which have better reservoir NMR characteristic quality, are concentrated mainly within the distributary channel and the upper shoreface environment which are the best in reservoir quality. In all, 69% of the samples from Relaxivity Groups 1 and 2 are from the distributary channel. The majority of samples from Relaxivity Group 3 are from the upper shoreface environment. The poorest reservoir quality samples are among Relaxivity Groups 6 through 8, which are found mostly in low current energy environments such as the lower shoreface and distributary mouth bar environments.

Grain Size and NMR Relaxation Groups

The textural information, based on 55 selected samples examined petrographically, also supports the observations seen in the depositional environment analysis. The lowest Relaxivity Group numbers have the highest estimated average particle size. High-energy distributary channel and upper shoreface samples are typically coarser grained than samples from lower energy environments. From Figure 7, it is shown that medium- and coarse-grained sandstones are concentrated in Relaxivity Groups 1 and 2, while very fine-grained sandstones are concentrated in the higher Relaxivity Group numbers. For these samples, 90% of all medium-grained sandstones are found in Relaxivity Groups 1-3. About 61% of the very fine-grained sandstones fall within the Relaxivity Groups 4 and 5. Fine-grained sandstones have a more even spread in all Groups. This relationship is also expressed in Figure 6 which shows that the higher Relaxivity Group numbers (6 to 8) have greater than 5 weight percent clay and are generally fine-grained or finer. For samples with less than 5% clay, the texture of the sample is directly proportional to reservoir quality and fall within low Relaxivity Group numbers. The coarser grained samples that fall within the higher Relaxivity Group numbers or lower reservoir quality samples generally have secondary factors affecting their reservoir quality such as carbonate cement or clay content.

Iron-bearing Minerals and NMR Relaxation Groups

Based on the 55 samples examined petrographically, iron-bearing minerals were also found to play an important role in influencing Relaxivity Group number. The most common iron-bearing minerals in these samples are siderite, pyrite, and illitic clay. Minor to trace amounts of jarosite also contain iron, but this is an insignificant amount relative to the other iron minerals. Figure 8 shows that almost all of the samples examined from Relaxivity Groups 1 to 4 have less than 3% iron-bearing minerals. In contrast, Relaxivity Groups 5 to 8 have less than 50% of the samples with less than 3% iron-bearing minerals. Commonly, samples within Relaxivity Groups 5 and higher have greater than 10% iron-bearing minerals in the form of illitic clay, siderite, and pyrite. Primary rather than secondary effects control this relationship, because most of the illite, siderite and pyrite are associated with detrital clay matrix, which is controlled by the depositional environment. Most of the illite is in the form of detrital clay and the siderite occurs as a replacement product of the detrital clay matrix.

In summary, the Relaxivity Groups in this example are influenced by primary depositional factors more so than by secondary effects. Higher flow regime samples are concentrated in the low Relaxivity Group numbers and are characterized by medium- and coarse-grained sandstones with low clay content, contributing to a pore network dominated by primary and well-interconnected pores. Low flow regime samples such as lower shoreface and shelf environments are generally very fine-grained, have high detrital clay content with associated pyrite and siderite and have a higher percentage of ineffective micropores in addition to any other pore types present.

RESULTS OF EXAMPLE 2

In another study performed with 18 sandstone rock samples from a North American field, three relaxivity groups were identified as shown in Figure 9. The NMR characteristics of the groups are presented in Table 3. The core samples used in the study were selected to cover the mineralogical and textural changes in the well, which penetrated two formations at depth intervals 6000-7200 ft and 9400-9470 ft. The values of ρ_2 , S_{gv} and R_{pt} were computed in a similar manner as in Example No. 1. The plot of r_{mh}/F_z versus FZI, shown in Figure 10, yielded $t\sqrt{F_s} = 1.0$.

Cutoff Relaxation Time and Non-movable Porosity

Like in Example 1 average values of T_{2c} per relaxivity group increase with $1/\rho_2 S_{gv}$ as presented in Table 3. The T_{2c} measurements were made on 14 of the 18 samples studied. As can be seen from Table 3 there is a defined relationship between the T_{2c} and relaxivity groups.

FZI-BVI RELATIONSHIP

FZI has previously been shown^{2,3,4} to have a non-linear relationship with non-movable saturation, and therefore with BVI ($S_{wirr}=BVI/\phi$). FZI values were calculated from core analysis data and used with the non-movable porosity determined from NMR measurements of the desaturated samples to develop a model for the FZI-BVI relationship. The FZI-BVI relationship is typically of the following general form:

$$FZI_{NMR} = \left[\frac{b(1.0 - \frac{NMRBVI}{f})}{1.0 + a(\frac{NMRBVI}{f} - 1)} \right]^c \quad (12)$$

In both examples the coefficients a, b, and c in equation (12) were obtained by non-linear regression on the core FZI-BVI database. The FZI-BVI relationship for each EOD and for the entire region in Example No. 1 is shown in Figure 11. In Example No. 2 the two formations were modeled separately. The FZI-BVI relationships are shown in Figure 12. The values for the coefficients are tabulated below:

Example 1: EOD	a	b	c	Example 2: Formation	a	b	c
1 – Channel Sand	1.0	1.0	1.0	6000-7200 feet	1.22	0.186	0.71
2 – Upper/Middle Shoreface	1.0	1.0	1.0				
3 – Lower/Middle Shoreface	0.9	1.0	1.0				
4 – Other Sands	1.01	0.75	0.5	9400-9470 feet	1.041	1.305	0.94
Entire Region	1.0	1.0	1.0				

PERMEABILITY MODELS

The FZI models derived from equation (12) are used in the following equation for permeability prediction from NMR log data.

$$K_{NMR} = 1014 \times FZI_{NMR}^2 \frac{f_{NMR}^3}{(1 - f_{NMR})^2} \quad (13)$$

All parameters in equation (13) are obtained from NMR logging. And thus, with appropriate calibration using laboratory core NMR data, permeability can be estimated from NMR logs. Figure 13 shows the comparison between the core-measured permeability and the core permeability calculated using NMR models (including equations 12 and 13) for the entire region in Example No. 1. A good match was also achieved between the core-measured permeability and modeled core permeability for Example No. 2.

CONCLUSIONS

1. It has been demonstrate that identification and delineation of NMR relaxivity groups provide for proper application of laboratory NMR calibration data to log analysis.
2. There is a correlatable relationship between T_2 cut off and relaxivity groups as validated with two example studies.
3. Permeability model based on variable T_2 cut off assigned per relaxivity group provides a better match of measured and predicted permeabilities than the empirical single T_2 cut off of 33 ms for sandstones.
4. There is a direct relationship between NMR facies and geological facies: good reservoir NMR characteristic quality are mainly found within the high current energy environments such as the distributary channel and the upper shoreface environment which are the best in reservoir quality.

RECOMMENDATIONS

1. Use of laboratory NMR calibration data in log analysis is recommended to correctly identify and delineate relaxivity groups or NMR facies.
2. The relaxivity grouping method allows direct application of laboratory based model for log interpretation irrespective of tool dependent factors like logging speed, borehole conditions, fluid types and saturation.
3. The following procedure is recommended for applying core calibration data to NMR logs:
 - (a) Find the relaxation group for the logged zone by dividing its log-median NMR T_2 expressed in seconds by the NMR-derived porosity group $\Phi_{\text{NMR}} = \phi_{\text{NMR}} / (1 - \phi_{\text{NMR}})$.
 - (b) Use appropriate core calibration data of T_{2c} to determine BVI from the log data in each relaxivity group.
 - (c) Use equations (12) and (13) to compute FZI_{NMR} and permeability, respectively.

NOMENCLATURE

- T_2 = NMR transverse relaxation time, t, ms, s.
 ϕ_z = porosity group, fraction
 ρ_2 = rock surface relaxivity, L^2/t , $\mu\text{m}^2/\text{s}$
 S_{gv} = specific rock surface area, L^2 , μm^2
 ϕ = porosity, fraction, %.
 T_{2c} = NMR T_2 cut off, t, s.
 r_t = pore throat radius, L, μm
 r_{mh} = mean hydraulic radius, L, μm

ACKNOWLEDGMENT

The authors thank Core Laboratories for the permission granted to publish this manuscript. Additional thanks is due to all who participated in performing the laboratory tests at Core Laboratories' Dallas office including Dane Daneshjou, Gerry Wayne, Jennifer Cuttler and Don Harville.

REFERENCES

1. Marschall, D. M., and Coates, G.: "Laboratory MRI Investigation in the Effects of Invert Oil Muds on Primary MRI Log Determination," paper SPE 38739 presented at the 1997 SPE Annual Technical Conference and Exhibition held in San Antonio, Texas, 5-8 October 1997.
2. Amaefule J.O., Altunbay M., Tiab, D., Kersey, D.G., and Keelan, D.K.: "Enhanced Reservoir Description: Using Core and Log Data to Identify Hydraulic (Flow) units and predict permeability in uncored Intervals/Wells", paper SPE 26436, presented at the 68th Annual SPE conference and exhibition, Houston, Texas, October 3 - 6, 1993.
3. Martin, A. J. (Jeff), Solomon, S.T., and Hartmann, D.J.: "Characterization of Petrophysical Flow Units in Carbonate Reservoirs," AAPG Bulletin, V. 81, No. 5 (May 1997), p. 734-759.
4. Ohen, A. H., Ajufo, A., and Curby, F.: "A Hydraulic (Flow) Units Based Model for the Determination of Petrophysical Properties from NMR Relaxation Measurements," paper SPE 30626 presented at the 1995 SPE Annual Technical Conference and Exhibition held in Dallas, Texas, 22-25 October 1995.
5. Ohen, A. H., Ajufo, A., and Enwere, M. P.: "Laboratory NMR Relaxation Measurements for the Acquisition of Calibration Data for NMR Logging Tools," paper SPE 35683 presented at the SPE Western Regional Meeting held in Anchorage, Alaska, 22-24 May 1996.
6. Geogi, D. T. and Menger, S.K.: "Reservoir Quality, Porosity and Permeability Relationships," Paper presented at the Mintrop Seminar Germany, May 1994.

	Group-1	Group-2	Group-4	Group-5	Group-6	Group-7	Group-8
Mean	1.163	0.576	0.252	0.148	0.071	0.031	0.011
Standard Error	0.111	0.015	0.005	0.003	0.002	0.001	0.001
Median	0.968	0.546	0.249	0.145	0.072	0.030	0.011
Standard Deviation	0.442	0.102	0.035	0.029	0.016	0.009	0.005
Skewness	2.965	0.850	0.279	0.293	0.160	0.344	0.192
Range	1.786	0.348	0.109	0.097	0.058	0.025	0.018
Minimum	0.888	0.445	0.205	0.104	0.046	0.020	0.002
Maximum	2.674	0.793	0.313	0.201	0.103	0.045	0.020
Sum	18.611	25.930	13.596	11.547	3.813	1.032	0.647
Count	16	45	54	78	54	33	59
Confidence Level (95%)	0.217	0.030	0.009	0.007	0.004	0.003	0.001

Relaxation Group	T_2 Median	RQI	NMR ϕ	$1/\rho_2 S_{gv}$	ρ_2	S_{gv}	r_p	T_{2c}	R_{pt}	r_t
	ms	μm	%	s	cm/s	cm ⁻¹	μm	ms		μm
1	301.78	4.489	20.62	1.163	0.005	162.818	50.766	41.250	1.584	32.048
2	173.18	3.070	22.67	0.576	0.006	275.805	47.056	31.389	1.888	24.928
3	116.08	2.831	23.52	0.369	0.009	312.581	34.911	22.500	2.598	13.439
4	83.23	2.597	24.26	0.252	0.011	358.518	17.455	20.357	3.323	5.252
5	49.33	2.013	24.64	0.148	0.014	466.393	14.432	16.893	4.345	3.321
6	23.44	1.370	24.24	0.071	0.021	682.674	4.521	14.250	6.224	0.726
7	9.75	0.700	22.96	0.031	0.025	1254.546	0.525	9.778	7.647	0.069
8	3.27	0.465	22.06	0.011	0.050	1808.542	1.268	9.000	15.137	0.084

DEPTH	Sample ID	Ka	RQI	NMR ϕ	T_2 Median	$\rho_2 S_{gv}$	$1/\rho_2 S_{gv}$	ρ_2	S_{gv}	T_{2c}	r_p	R_{pt}	r_t	
		mD	μm	%	ms	s ⁻¹	s	cm/s	cm ⁻¹	ms	μm		μm	
	9458.6	26	136.58	0.725	25.60	60.00	5.735	0.174	0.00363	1582.005	20	6.525	2.533	2.575
	9460	27	121.72	0.747	21.50	28.60	9.576	0.104	0.00784	1222.157	20	6.723	2.462	2.730
	6132.5	8	18.42	0.285	22.40	29.30	9.852	0.102	0.00292	3376.138	19	2.565	5.502	0.466
	6087.8	3	14.58	0.256	21.90	24.90	11.261	0.089	0.00308	3651.168	20	2.304	5.861	0.393
Averages	→		72.83	0.503	22.85	35.70	9.106	0.117	0.004	2457.867	20	4.529		1.541
	9445.5	22	138.76	0.714	26.80	22.00	16.642	0.060	0.00974	1709.245	18	6.426	2.569	2.500
	9415.5	15	4.30	0.157	17.10	12.00	17.189	0.058	0.00393	4379.461	18	1.413	6.976	0.202
	7138	9	0.80	0.065	18.5	11.70	19.401	0.052	0.00167	11640.711	18	0.585	5.410	0.108
	9435	19	2.21	0.115	16.40	7.80	25.150	0.040	0.00442	5686.152		1.035	6.919	0.150
	7189	13	0.33	0.043	17.70	6.40	33.604	0.030	0.00202	16671.847		0.387	3.937	0.098
	7165.1	11	0.53	0.053	18.50	6.70	33.880	0.030	0.00237	14276.344		0.477	4.670	0.102
	7190	14	0.40	0.045	19.60	7.10	34.335	0.029	0.00190	18057.859	18	0.405	4.104	0.098
	7147	10	0.43	0.048	17.9	5.30	41.137	0.024	0.00272	15140.750		0.432	4.361	0.100
Averages	→		18.47	0.155	19.06	9.88	27.667	0.040	0.004	10945.296	18	1.395		0.420
	6085.6	2	4.66	0.138	24.00	6.18	51.099	0.020	0.00670	7627.765	10	1.242	7.036	0.177
	6079.3	1	3.42	0.125	21.50	5.35	51.194	0.020	0.00701	7303.609	7	1.125	1.869	0.161
	9431.5	17	39.49	0.426	21.50	5.10	53.703	0.019	0.02506	2143.078	5	3.834	6.682	0.939
	9433.4	18	10.35	0.261	15.00	2.40	73.529	0.014	0.03263	2253.775		2.349	5.802	0.405
	9429.5	16	25.71	0.346	21.20	3.60	74.732	0.013	0.02883	2591.864	6	3.114	7.689	0.647
	6128.5	6	4.75	0.157	19.10	2.70	87.442	0.011	0.01744	5012.610	7	1.413	4.652	0.202
Averages	→		14.73	0.24	20.38	4.22	65.28	0.02	0.02	4488.78	7	2.18		0.42

FIGURE 1: NMR Core Analysis Procedure

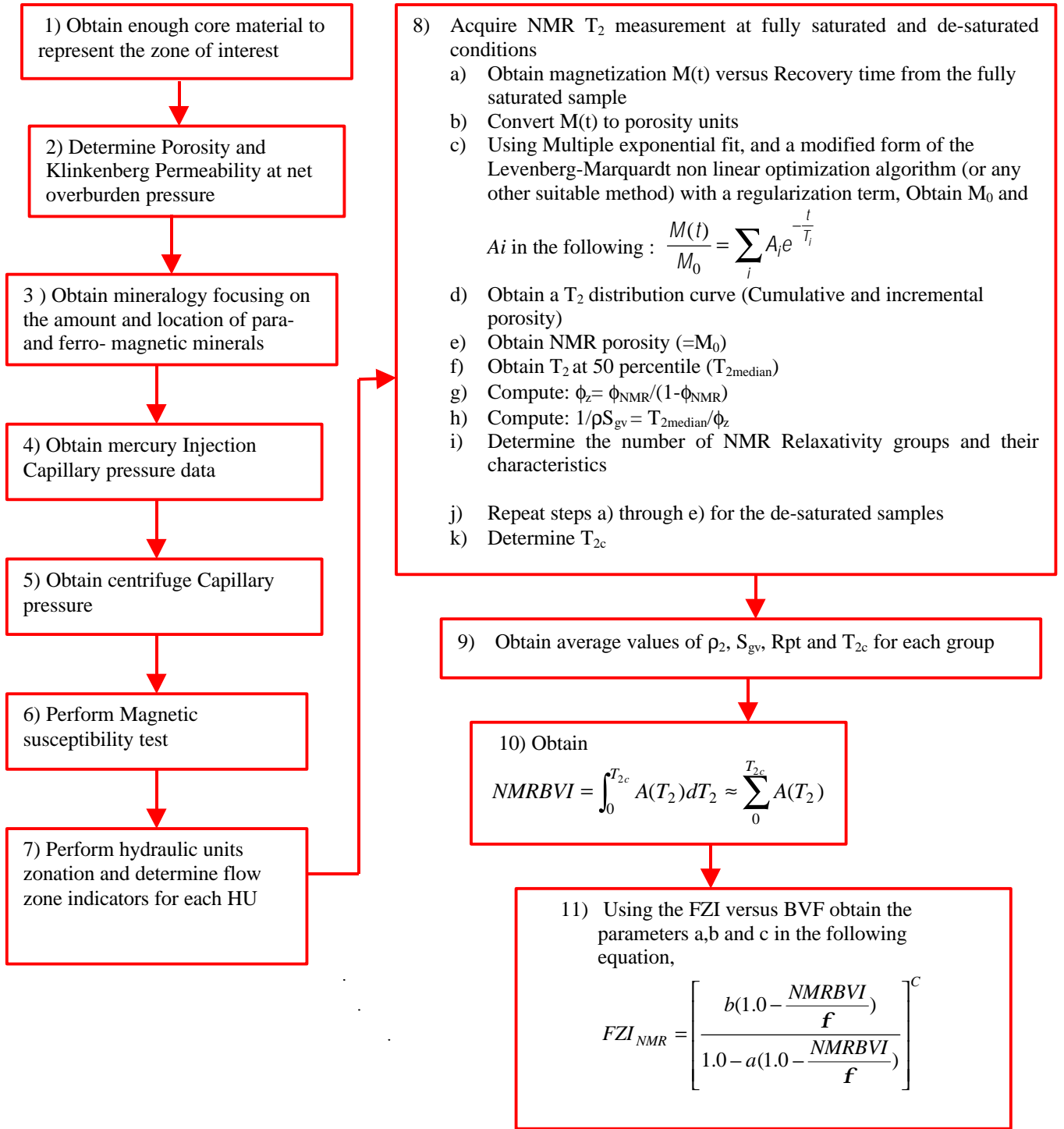


Figure 2: Tortuosity Constant Determination Plot- Gulf Coast Carbonate Example

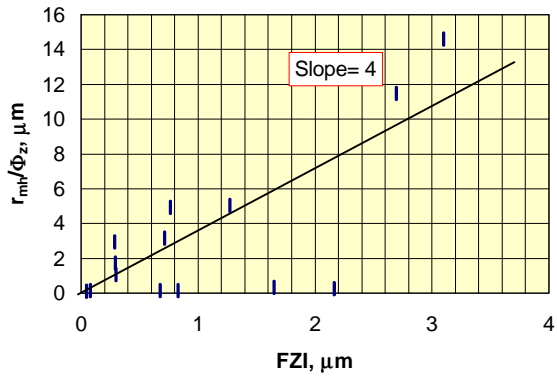


Figure 3: Relaxivity Grouping for Example No. 1

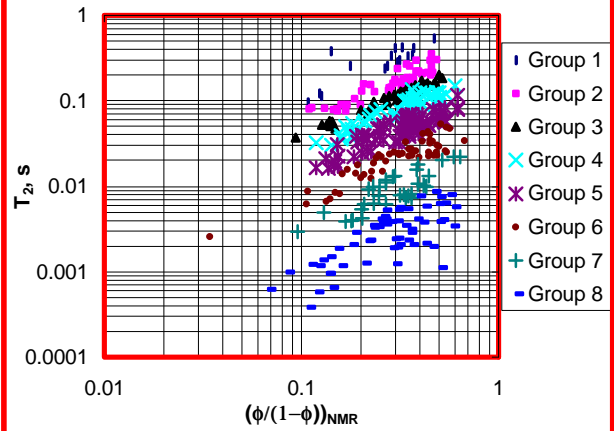


Figure 4: Pore Throat Radius/phi_z versus FZI for Example No. 1

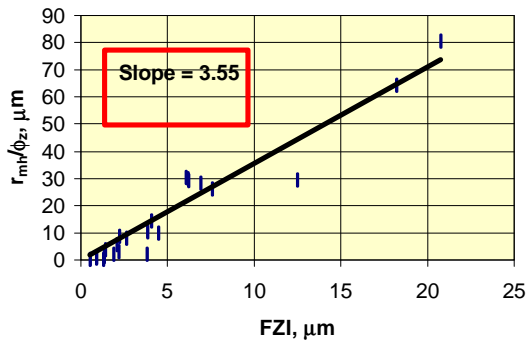


Figure 5: Variation of Pore Throat Size with T2 for Example No. 1

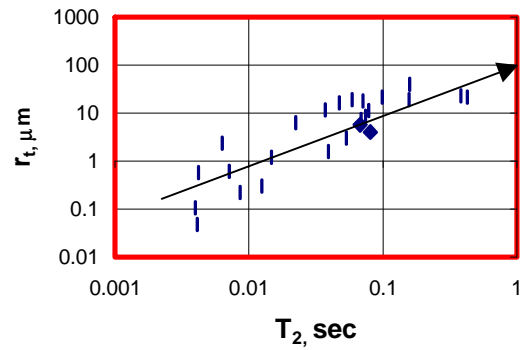


Figure 6: EOD vs. Relaxivity Group

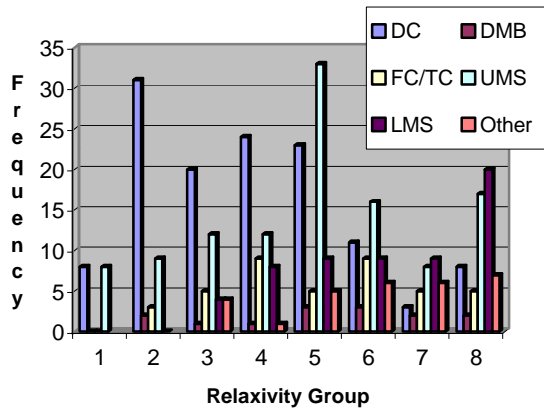


Figure 7: Texture vs. Relaxivity Group

